Optical Color Pattern Recognition Based on Linear Models of Surface and Illuminant Spectra

Juan L. Nieves, Javier Hernández-Andrés, Eva M. Valero, and Javier Romero
Departamento de Óptica. Facultad de Ciencias. Universidad de Granada
Granada, Spain

Abstract

Apart from shape and size, color is one of the most important characteristics in the discrimination and recognition of objects. The introduction of color information in optical pattern recognition is usually made via the multi-channel correlation technique, which decomposes the source and the target color images in three RGB channels. In this work we propose a new method for optical color pattern recognition based on the use of linear models that describe both the surface and the illuminant spectra, and we face the extension of correlation matched filter operations designed for pattern recognition. Different scenes were captured with a CCD camera and three correlation operations were used to test the model. The results show that the coefficient method derived from the linear description of images can discriminate polychromatic objects by optical correlation and leads to results that are almost independent of any spectral change in the illuminant. The discrimination capability of this method is clearly an improvement upon that obtained with the RGB multi-channel decomposition and is slightly better than other approaches used in optical correlation which are based on uniform color spaces. The method allows the use of more than three "color" components in optical pattern recognition, which can lead to better spectral surface description and accurate color object recognition.

Introduction

The introduction of color information in optical pattern recognition is usually made via the multi-channel correlation technique, which decomposes the source and the target color images in three RGB (red-green-blue) channels.[1-3] The correlation is made separately for each channel and arithmetic or logical point-wise operations can be used to derive the final output. A common way in which objects are optically recognized is by use of a multi-channel joint transform correlator where filters matched to the target are used in each channel.[4] Different methods have been proposed to enhance the differences between the images of each channel to achieve better recognition.[5-7] Some of these transformations benefit of color vision models and increase discriminability when they are compared to the RGB transformation. They avoid false alarms for equal shape objects but different in color and even reduce the number of effective channels contributing to color correlation.[8] But only a few studies addressing the problem of finding optical pattern recognition architectures that are not susceptible to changes in the illuminant have been published.[9-10] One of the latest works have considered the use of uniform color spaces, such as the CIELab, which are more stable in the face of these changes. The correlation made in the luminance, chroma and hue channels provide better discrimination capability than conventional RGB techniques, and the use of only two channels (the luminance and the hue channels) simplifies the recognition process providing recognition results stable under changes in the illuminant.[10]

Color pattern recognition can also be achieved from computational algorithms that are color constant. For example, color indexing involves matching color space histograms and departs from another recognition techniques based on geometrical properties of objects.[11-13] Objects are identified by comparing their color components to the color components of each object in a pre-defined database; the intersection of histograms is usually used to recognize the color object. Before histogramming, illuminant-invariant descriptors can be defined to derive pattern recognition independent of illuminant changes.[11] Whereas optical pattern recognition seeks for correlation peaks that correspond to the spatial position of the target in the image, computational color constancy algorithms usually recover an illuminant independent representation of the color images or the retrieval of images from large collections of image database.[12-13]

In the context of this paper we show how linear models of surface and illuminant spectra coupled with optical correlation architectures can be used to discriminate objects of the same shape but different in color.[14] Our algorithm simulates a multi-channel optical correlator where the correlation is made throughout the spatial distribution of the coefficients derived from the linear representation of each reflectance function in an appropriate basis.

Background

According to basic concepts of image acquisition, an image taken with a digital camera can be decomposed into N channels described by:

$$I_N(x,y)=\sum_\lambda q_N(\lambda)S(x,y,\lambda)E(x,y,\lambda)\Delta\lambda \qquad (1)$$

where N represents each of the camera channels, $q_N(\lambda)$ is the spectral sensitivity of each channel (e.g. N = 3 for conventional CCD color cameras), S(x,y, λ) the spectral reflectance function at pixel (x,y) and E(x,y, λ) the spectral power distribution (SPD) of the illuminant under which the image is captured at pixel (x,y); in the following we will be assumed that images are uniformly illuminated and the dependence of illumination with (x,y) will be omitted. By assuming that both illuminants and surfaces are constrained to lie within small-dimensional linear models, equation (1) can be rewrite as

$$I_N(x,y)=\sum_{i=1}^{m}\sum_{j=1}^{n}\sigma_j(x,y)\varepsilon_i\gamma_{ijN} \qquad (2)$$

where

$$\gamma_{ijN}=\sum_\lambda q_N(\lambda)S_j(\lambda)E_i(\lambda)\Delta\lambda$$

and $E_i(\lambda)$ and $S_j(\lambda)$ are the eigenvectors that describe the SPD of the illuminant and the surface reflectance, respectively.[15] Thus each image pixel can be characterized through a set of coefficients σ_j^{xy} as

$$\sigma^{xy}=\Lambda_\varepsilon^{-1}I_N^{xy} \qquad (3)$$

This expression allows to decompose the input image into N channels and avoids the dependence with the illuminant conditions for the basis selected.

Methods

Based on the above description of the multi-channel transformation of the image, the optical recognition process can be achieved from the finite subspace of the σ^{xy} coefficients and the matched filter operations usually applied in optical pattern recognition can be generalized. Let $\sigma_s(x,y)$ and $\sigma_t(x,y)$ represent the input coefficients associated to the source image and the impulse response of a Fourier filter associated to the target to be discriminated, respectively. The correlation between the transformed color image and the filter impulse response is defined as,

$$c_\sigma(x,y,j)=\sum_{x'=0}^{dx-1}\sum_{y'=0}^{dy-1}\sigma_s(x,y,j)\sigma_t^*(x'-x,y'-y,j) \qquad (4)$$

where dx and dy are the dimensions of the image, and *j* is the number of channels (dimension of the surface reflectance basis), which are processed independently. The multichannel correlation expressed by equation (4) and the linear filtering derived from it could be implemented in a classical correlator architecture following the scheme described in figure 1. The output is derived from an arithmetic or logical operator (i.e. square summation rule, AND, etc.) and the obtained correlation peak signals the position of the target in the scene.

It is clear from equation (3) that we need an estimation algorithm of the illumination to derive the illuminant matrix Λ_ε and to solve for coefficients σ_j^{xy}. To clearly state the potential use of the optical correlation method proposed here we will assume either one of the simplest illuminant estimation hypothesis or controlled illuminant conditions. So we will consider one of the simplest illuminant estimation hypothesis found in the literature to test the correlation results derived from the multi-channel transformation associated to equation (4) since it suffices to obtain good discrimination results by optical correlation. This hypothesis makes use of a reference white, which will be a diffuse white surface and must be placed within the scene to be captured. Following the linear description of surfaces and illuminants derived from equations (1)-(3) the intensity of the multi-channel image of the white surface can be expressed as

$$\begin{aligned}I_{N,W}(x,y)&=\sum_\lambda\sum_{i=1}^{m}S_W(x,y,\lambda)\varepsilon_iE_i(\lambda)q_N(\lambda)\Delta\lambda=\\&=\sum_{i=1}^{m}\varepsilon_i\left[\sum_\lambda S_W(x,y,\lambda)E_i(\lambda)q_N(\lambda)\Delta\lambda\right]\end{aligned} \qquad (5)$$

where $S_W(x,y,\lambda)$ is the a priori known reflectance of the white surface placed at co-ordinates (x,y). The factor inside the brackets contains only fixed elements which are independent of the image once a suitable basis of linear representation of illuminants has been selected. The quantities $I_{N,W}(x,y)$ are all known from the location of the white surface in the captured image. Thus, if the number of channels that specifies the image is $N=m$, the linear system of equations (5) can be solved for each ε_i, and by incorporating the obtained coefficients in equations (3) we can recover the coefficients σ_j^{xy} for each image pixel.

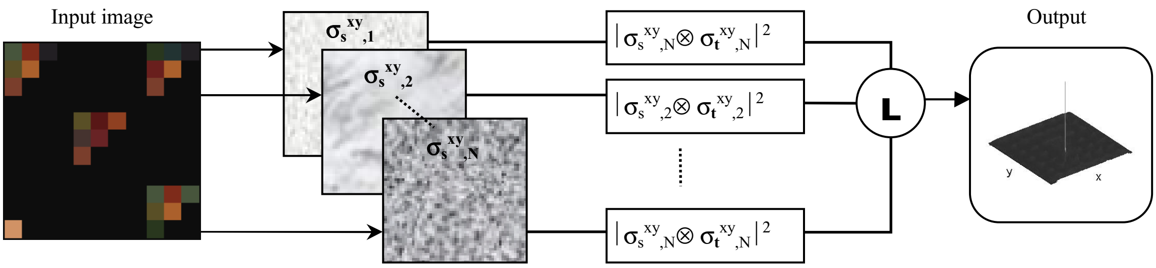

Figure 1. Scheme of the optical correlation based algorithm proposed. The output is derived from an arithmetic or logical operation **L** *(i.e. addition, AND, etc.) applied to the multiple input channels; the symbol ⊗ means correlation.*

Other more elaborated illuminant estimation approaches has been proposed in the literature which benefits of image statistics, scenes averages, highlights, etc. The purpose of our work is not to develop a color constant image but to benefit of these color constancy algorithms to obtain correlation peaks invariants to the changes in the illuminant.

Results

1. Discrimination of Color Objects in Simulated Scenes

Since optical correlation depends strongly upon the spatial characteristics of the objects to be discriminated, we test our method with input images that contained different objects of the same shape but different in color (figure 2); in addition, the colored areas of object O4 were selected in such a way that the differences in RGB components compared to O1 were small under each of the test illuminants used. The scenes were captured under different test illuminants with a CCD color camera (JVC TK-1270E), and thus N = 3 in the following calculations. To test the algorithm we fixed the dimension of the bases at n=3, which corresponds to the same number of RGB channels. To estimate the illuminant the reference surface was placed in the lower left corner of the scene (see figure 2); the white reference surface was the chip number 19 of the GretagMacbeth ColorChecker. Two kinds of images were captured in the experiment: the target image with 65 x 65 pixels, which was always captured under the D65 illuminant, and the source image with 230 x 230 pixels, which was captured under four unknown test illuminants. The object O1 in figure 2 was the target when the scene was captured under the illuminant D65; it can be seen how the target within the source scene visually changed under the two different illuminant conditions.

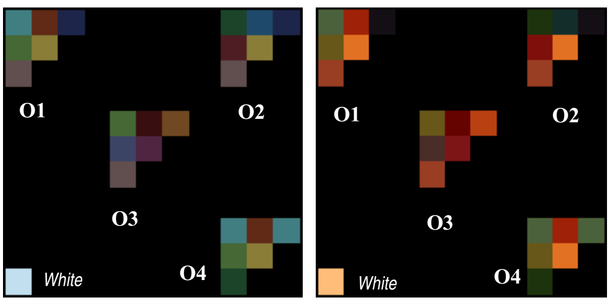

Figure 2. Input color image captured under (left) D65 illuminant and (right) one of the test illuminants.

We performed three different numerical correlations. First, we used the RGB multi-channel decomposition, which transform the color images into the three R, G and B color channels and correlates each channel independently.[2] Second, we used the CIELab multi-channel decomposition where the RGB components of input scenes are transformed to three L*, a* and b* color components.[9] Third, we performed our multi-channel decomposition expressed in terms of three coefficients σ_1^{xy}, σ_2^{xy}, and σ_3^{xy}. In all cases the correlation was made separately for each channel and the AND logic operator was applied with the usual threshold of 50% of the maximum as the positive discrimination threshold.[14]

The equation (3) was used to transform the color images under each of the unknown illuminants and to recover the coefficients σ_j^{xy}. The correlation was performed between these coefficients and the corresponding ones of the target. The results are summarized in Table 1 for the three multi-channel techniques and two of the test illuminants. On one hand, the results show the poor discrimination of the RGB multi-channel correlation since it identifies the O1 and the O4 as the target for all the test illuminants. When we use the CIELab system the results are satisfactory and only present a false alarm for object O1, O3 and O4 under the test illuminant 4. On the other, the illuminant estimation hypothesis and the method of coefficients provide enough discrimination to recognize O1 under all the test illuminants, even though the color appearance of the target under the reference illuminant D65 (O1 in the upper left corner in Fig. 2a) was completely different from its corresponding image under each of the unknown illuminations (e.g. O1 in Fig. 2b under test illuminant 4). This result confirms the good discrimination capability of the proposed algorithm independently of the spectral changes in the illumination. Figure 3 show examples of the correlation results derived from the CIELab system and the coefficients σ_1^{xy}, σ_2^{xy} and σ_3^{xy} when the source image was captured under one of the test illuminants.

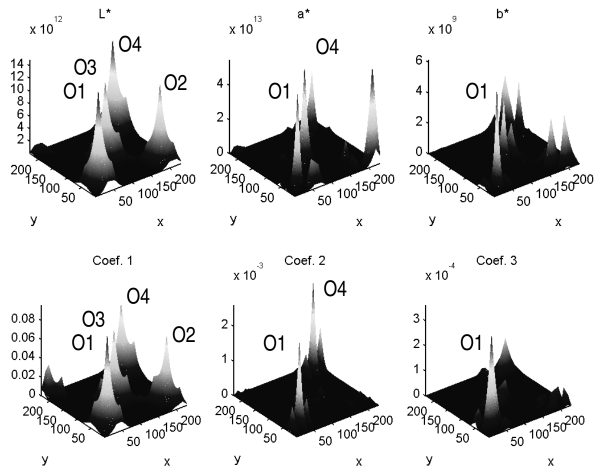

*Figure 3. Correlation peaks derived from the L*a*b* components (upper row) and the coefficients σ_1^{xy}, σ_2^{xy}, and σ_3^{xy} (lower row) when the scene was captured under the test illuminant 4 and the target O1 under the D65 illuminant. The x and y co-ordinates represent spatial positions in the image. The position of the target within the image is indicated by the existence of the prominent peak O1 in all the three coefficient planes.*

Table 1: Correlation and discrimination results obtained using the RGB, the CIELab and the coefficient multi-channel decompositions under two test illuminants. The target is object O1 under the D65 illuminant. The threshold values at 50% of the maximum are also shown.

		Object				
Illuminant	**Channel**	**O1**	**O2**	**O3**	**O4**	**Thr. 50%**
Test 1	**R**	*5,356E+14*	*3,583E+14*	*3,286E+14*	*4,093E+14*	2,678E+14
	G	*3,506E+14*	1,893E+14	1,513E+14	*3,882E+14*	1,941E+14
	B	*8,047E+13*	3,983E+13	4,351E+13	*9,074E+13*	4,537E+13
Recog. (AND)		***YES***	NO	NO	***YES***	
Test 4	**R**	*2,626E+14*	*1,759E+14*	*1,755E+14*	*1,966E+14*	1,131E+14
	G	*9,639E+13*	5,274E+13	4,263E+13	*1,059E+14*	5,296E+13
	B	*1,777E+13*	*9,175E+12*	*1,060E+13*	*1,976E+13*	9,875E+12
Recog. (AND)		***YES***	NO	NO	***YES***	
		Object				
Illuminant	**Channel**	**O1**	**O2**	**O3**	**O4**	**Thr. 50%**
Test 1	**L***	*1,534E+13*	*1,249E+13*	*1,190E+13*	*1,359E+13*	7,669E+12
	a*	*1,121E+14*	1,666E+13	5,042E+13	*8,032E+13*	6,060E+13
	b*	*7,522E+09*	2,991E+09	*4,368E+09*	3,332E+09	3,771E+09
Recog. (AND)		***YES***	NO	NO	NO	
Test 4	**L***	*1,492E+13*	*1,217E+13*	*1,216E+13*	*1,435E+13*	7,461E+12
	a*	*5,331E+13*	*5,466E+13*	*5,270E+13*	*3,458E+13*	2,733E+13
	b*	*6,154E+09*	3,056E+09	*3,785E+09*	*3,370E+09*	3,077E+09
Recog. (AND)		***YES***	NO	***YES***	***YES***	
		Object				
Illuminant	**Channel**	**O1**	**O2**	**O3**	**O4**	**Thr. 50%**
Test 1	**Coef. 1**	*1,105E-01*	*8,050E-02*	*8,261E-02*	*8,371E-02*	5,525E-02
	Coef. 2	*2,870E-03*	2,135E-05	4,405E-05	*3,110E-03*	1,550E-03
	Coef. 3	*4,646E-04*	6,796E-05	6,240E-05	1,853E-04	2,320E-04
Recog. (AND)		***YES***	NO	NO	NO	
Test 4	**Coef. 1**	*9,616E-02*	*7,111E-02*	*7,481E-02*	*7,331E-02*	4,810E-02
	Coef. 2	*2,418E-03*	1,264E-05	1,552E-04	*2,604E-03*	1,300E-03
	Coef. 3	*3,621E-04*	3,820E-05	5,628E-05	1,416E-04	1,810E-04
Recog. (AND)		***YES***	NO	NO	NO	

2. Discrimination of Color Objects in Real Scenes

Next we show examples of the discrimination results derived from real scenes to prove the validity of the algorithm. The digital GretagMacbeth ColorChecker was captured in a lighting cabinet under a daylight D65 simulator; the time exposure was adjusted before image capturing to discard any saturated digital counts. First we captured the target labeled as O1 in the figures 4 and 5 by covering the rest of color areas in the ColorChecker with a black paper. Then both the target and the source images were transformed independently according to equation (3) and the correlation described by the multi-channel equation (4) was obtained. The illuminant estimation was derived from the white area in the center of the image. The figure 4 resumes the discrimination results from each of the coefficients σ_1^{xy}, σ_2^{xy} and σ_3^{xy}; in this case we have normalized to unity the correlation planes for clarity. After applying the AND operator to the three planes the coefficient correlation method leaded to a positive discrimination of each of the color objects O1.

For real color objects it is clear from the figures that additional peaks appear around the target; however none of them lead to false alarms. This is because color capturing with a CCD is a noisy process even when the camera is carefully calibrated and the dark noise is appropriately subtracted from the RGB values of each pixel. Also the results suggest that the linear models of reduced dimension used here probably do not suffice for an adequate description of surface reflectances. It is important to analyze in future studies the use of multispectral object recognition with more than three coefficients, as we commented before, and its influence in the design of the matched filters used in the optical correlation architecture.

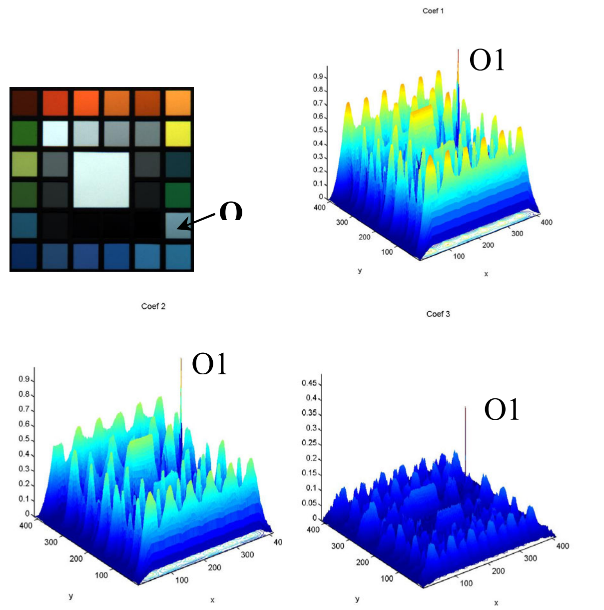

Figure 4. Source image and correlation peaks derived from the coefficient correlations when the color object O1 was captured under the D65 illuminant. The position of the target within the image is indicated by the maximum peaks O1 in the correlation planes σ_1^{xy}, σ_2^{xy} and σ_3^{xy}.

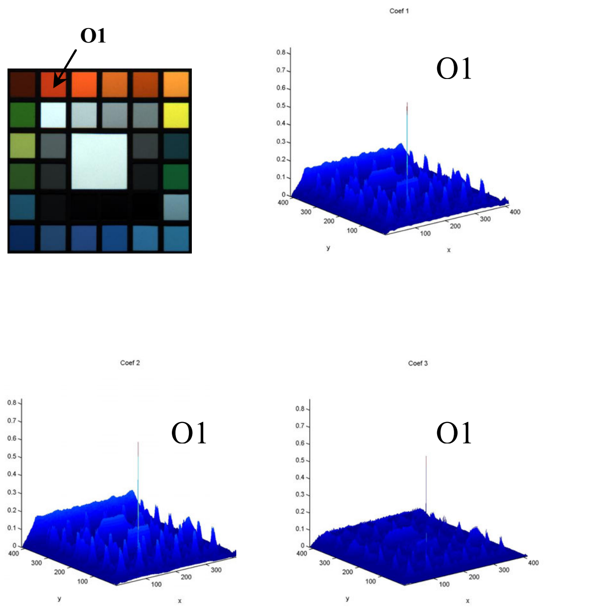

Figure 5. Source image and correlation peaks derived from the coefficient correlations when the color object O1 was captured under the D65 illuminant. The position of the target within the image is indicated in this case by the maximum peaks O1 in the correlation planes σ_1^{xy}, σ_2^{xy} and σ_3^{xy}.

Conclusions

The use of linear models to describe the color input images leads to a multi-channel optical correlation of range as higher as the dimension of the bases chosen to describe the surfaces and illuminants. The additional advantage of the coefficient correlation is that once the linear basis has been selected, it allows the user to transform the input image into a subspace where the spatial information is preserved and the dependence upon the spectral content of the illumination is discarded. Thus the algorithm offers a new possibility to overcome the problems derived from filter design in optical correlation architectures when the source and target images are captured under different illuminant conditions. Since many objects and illuminants can be described by linear models of a reduced dimension the method can optimize the polychromatic object discrimination even in real images.

References

1. F.T.S. Yu, Opt. Eng. 23, 690-695 (1984).
2. M.S. Millán, J. Campos, C. Ferreira and M.J. Yzuel, Opt. Commun. 73, 277-284 (1989).
3. M.S. Millán, M. Corbalán, J. Romero and M.J. Yzuel, Opt. Lett. 20, 1722-1724 (1995).
4. M.-L. Hsieh, K.Y. Hsu and H. Zhai, Appl.Opt. 41, 1500-1504 (2002).
5. I. Moreno, V. Kober, V. Lashin, J. Campos, L.P. Yaroslavsky and M.J. Yzuel, Opt. Lett. 21, 499-500 (1992).
6. M.S. Millán, M. Corbalán, J. Romero and M.J. Yzuel, Opt. Lett. 20, 1722-1724 (1995).
7. A. Fares, P. García-Martínez, C. Ferreira, M. Hamdi and A. Bouzid, Opt. Commun. 203, 255-261 (2002).
8. M. Corbalán, M.S. Millán and M.J. Yzuel, Opt. Eng. 41, 130-138 (2002).
9. M. Corbalán, M.S. Millán and M.J. Yzuel, Opt. Eng. 39, 1470-1476 (2000).
10. M. Corbalán, M.S. Millán and M.J. Yzuel, Opt. Eng. 41, 130-138 (2002).
11. M.J. Swain and D.H. Ballard, Int. J. Comput. Vision, 7, 11-32 (1991).
12. B.V. Funt and G.D. Finlayson, IEEE Trans. Pattern Analysis and Machine Intelligence, 17, 522-529 (1995).
13. G.D. Finlayson, S.D. Hordley and P.M. Hubel, IEEE Trans. Pattern Analysis and Machine Intelligence, 23, 1209-12221 (2001).
14. J.L. Nieves, J. Hernández-Andrés, E. Valero and J. Romero, Appl. Opt., in press (2004).
15. L.T. Maloney, in K.R. Gegenfurtner & L.T. Sharpe [Eds] (1999), Color Vision: From Genes to Sharpe [Eds] (1999), Color Vision: From Genes to Perception. Cambridge, UK: Cambridge University Press, pp. 387-422.

Biography

Juan L. Nieves received his B.S. degree in Physics from the University of Granada (Spain) in 1991 and a Ph.D. in Physics from the same university in 1996. Since 1992 he has worked in the Department of Optics at the Science Faculty, Granada. His work has primarily focused on the color vision and computer vision field, including color constancy, spatial vision and colorimetry. He is a member of the SPIE and the SEDO (Spanish Optical Society).